BIOCHEMISTRY
including biophysical chemistry & molecular biology

Article

pubs.acs.org/biochemistry

Mechanistic Insights into the Lipid Interaction of an Ancient Saposin-like Protein

Matthias Michalek* and Matthias Leippe

Zoological Institute, Comparative Immunobiology, University of Kiel, Olshausenstrasse 40, 24098 Kiel, Germany

ABSTRACT: The members of the expanding family of saposin-like proteins (SAPLIPs) have various biological functions in plants, animals, and humans. In addition to a similar protein backbone, these proteins have in common the fact that they interact with lipid membranes. According to their phylogenetic position, it has long been thought that amoeboid protozoans produce archetypes of SAPLIPs and that these are lytic proteins that can perforate membranes of prokaryotic and eukaryotic target cells. Here, we show that an amoebic SAPLIP from *Entamoeba invadens* does not form lytic pores in membranes but displays several characteristics that are known from human saposins. The protein named invaposin changes the conformation from a closed to an open form in the presence of lipid membranes, acts in a pH-dependent manner, selectively binds anionic lipids, aggregates lipid vesicles of the preferred composition, and dimerizes upon acidification. Our data indicate that the principal features of the lipid-binding saposins evolved long before the appearance of the vertebrate lineage and push the origin of saposins even deeper down the phylogenetic tree to unicellular organisms.

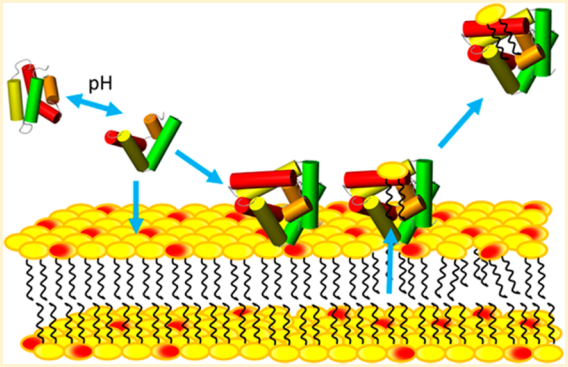

Saposin-like proteins (SAPLIPs) are members of a large protein superfamily that can be found in animals and plants. On the basis of a conserved fold, these proteins serve diverse functions but have in common the fact that they interact with lipids.[1,2] In humans, well-known examples are the eponymous saposins that arise from a common precursor and are pivotal cofactors of lipid-degrading enzymes inside cells. Mutations or deletions within the saposin precursor gene result in severe lipid storage diseases such as Gaucher disease or Krabbe disease.[3−5] Moreover, surfactant protein B is an essential component of the surfactant of the lung of neonates.[6] SAPLIPs are also involved in immunity: Saposin B and C participate in lipid antigen presentation by CD1 molecules,[7,8] and mammalian cytotoxic lymphocytes contain lytic SAPLIPs, namely, NK-lysin and granulysin, that kill microbes and cancer cells in that they permeabilize the membranes of the target cells.[9,10]

In recent years, accumulating structural information about selected SAPLIP members fulfilling the aforementioned functions gave detailed insights into the different molecular mechanisms of lipid interaction.[11−18] In particular, the three-dimensional structures of saposins in combination with lipids or detergents revealed a complex picture of lipid binding that is pH-dependent and lipid selective and comes along with oligomerization and conformational changes in the proteins.[15−17,19] It has been proposed that the inherent structural flexibility of saposins is decisive in allowing binding of the proteins to membranes and subsequent solubilization of lipids.[15−17,20]

Notably, SAPLIPs already existed before the advent of metazoa. In the amoebic protozoon *Entamoeba histolytica*, the causative agent of human amoebiasis, SAPLIPs coined "amoebapores" are pore-forming proteins that permeabilize membranes of engulfed bacteria and human host cells and are hence considered pathogenicity factors.[13,21] Similar proteins have been found in the amoebic protozoon *Naegleria fowleri*.[22] During a previous survey of amoebapore-like proteins in *Entamoeba invadens*, another amoeba that can cause a disease as severe as that caused by *E. histolytica* in reptiles and is well-known as a surrogate model for *Entamoeba* encystation in the laboratory,[23] we purified from amoebic extracts, and subsequently molecularly cloned, three isoforms of amoebapore-like proteins that we provisionally termed invapores (accession numbers AAP80379, AAP80380, and AAP80381). Intriguingly, whereas invapore A is the major pore-forming protein in extracts of *E. invadens*, another invapore isoform did not display any pore forming activity and was identified only upon screening for small cysteine-rich proteins by fluorescently labeling their cysteine residues.[24] Protein sequencing gave the first 20 residues starting with an N-terminal alanine, and molecular cloning yielded the complete coding sequence for the mature protein. It became evident that the natural protein is a nonglycosylated SAPLIP with the conserved array of six cysteine residues. The primary structure of the 78-residue polypeptide revealed that it is more hydrophilic than

Received: January 30, 2015
Revised: February 19, 2015
Published: February 26, 2015

DOI: 10.1021/acs.biochem.5b00094
Biochemistry 2015, 54, 1778−1786

amoebapores and that it possesses a large amount of acidic residues dispersed along the entire amino acid sequence. As these features are characteristic of true saposins rather than antimicrobial and lytic SAPLIPs, the question of whether amoebae, counter to intuition, contain a protein with properties known for the saposins such as selective lipid binding followed by lipid extraction arose.

Here, we report on the oligomerization and folding events that we observed in concert with a pH-dependent and selective lipid interaction of this particular amoebic protein that we name, in the following text, invaposin (INV).

For saposins, namely, saposins A, B, and C, there was a structural change observed between a closed form in solution and an open conformation in the presence of lipids.[15−17,20] As a consequence, it has been proposed that the inherent structural flexibility of saposins is necessary to allow binding of the proteins to membranes and subsequent solubilization of lipids.[14,25,26]

The location of two tryptophan residues at different positions within the polypeptide chain of invaposin made this protein particularly suitable to analyze, by fluorescence spectroscopy, whether conformational changes also occur in this molecule upon lipid interaction. Our data are consistent with the model of a conformational transition from a compact globular fold in solution to a V-shaped extension upon lipid interaction that might be the general principle for the lipid interacting properties of SAPLIP family members.

MATERIALS AND METHODS

All lipids and *Escherichia coli* lipid extracts were purchased from Avanti Polar Lipids (Otto Nordwald, Hamburg, Germany). LPS (from *E. coli*, 0111:B4), LDAO, SDS, alamethicin, cecropin P1, and melittin were from Sigma-Aldrich (Hamburg, Germany).

Recombinant Protein Production and Purification. The cDNA encoding invaposin was ligated into the pIVEX 2.4a (Roche, Mannheim, Germany) expression vector containing an ampicillin resistance gene using the *Ksp*I and *Nco*I restriction sites (pIVEX_INV). The expressed fusion protein contains an amino-terminal hexahistidine tag (His_6) and a factor Xa cleavage site preceding the primary structure of invaposin (underlined) as depicted below: MSGSHHHHHHSSGIEGR-GADPAVCSWCKTLIGQIEQLQAKHGRQTVEDYIDELCSI-ATDEALQVCKDWEAYGMSKVIDAIMAQEDPTAVCKAT-GSC. Factor Xa cleavage yielded a product in which the N-terminal alanine residue of INV is preceded by an additional glycine residue only.

For recombinant expression, the pIVEX_INV vector was transformed into *E. coli* BL21(DE3) and cultured in Luria-Bertani (LB) medium containing 100 μg/mL ampicillin, at 37 °C under shaking at 200 rpm. At an optical density at 600 nm (OD_{600}) of 0.6, protein expression was induced by addition of 1 mM IPTG (isopropyl β-D-1-thiogalactopyranoside). The bacterial culture was harvested after incubation for 4 h at 30 °C by subsequent centrifugation at 2500*g* and 4 °C for 15 min. Bacterial sediments were resuspended in ice-cold 50 mM sodium phosphate and 300 mM NaCl (pH 7.0) followed by sonication on a Bandelin Sonoplus sonicator (20% power with four cycles of 1 min). The resulting suspension was centrifuged at 40000*g* and 4 °C for 30 min, and supernatants were subjected to immobilized metal affinity chromatography using the TALON resin (Clontech, Saint-Germain-en-Laye, France). The fusion protein was eluted from the cobalt matrix using 50 mM sodium phosphate, 300 mM NaCl, and 150 mM imidazole (pH 7.8) and dialyzed twice against buffer without imidazole at 20 °C for 20 h. For disulfide reshuffling, 2 mM reduced glutathione and 0.2 mM oxidized glutathione were added to the sample chamber followed by two successive dialysis steps against buffer without glutathione for 20 h at 20 °C. The proteolytic cleavage of the fusion protein was performed using factor Xa protease (Roche, Mannheim, Germany) at 20 °C for 2 days followed by buffer exchange with 50 mM sodium acetate buffer (pH 4.0) using NAP-5 columns according to the manufacturer's instructions (GE Healthcare, Solingen, Germany). The cleavage products were separated on an equilibrated source 30S cation-exchange chromatography column connected to an Aekta Purifier System (GE Healthcare). Bound proteins were eluted using a 1%/min gradient of 50 mM sodium actetate and 1 M NaCl (pH 4.0) at a flow rate of 1 mL/min and 4 °C. Fractions containing invaposin were subjected to reverse phase high-performance liquid chromatography using a Vydac C18 column and an 84% (v/v) acetonitrile/water mixture containing 0.1% (v/v) TFA. The fraction of invaposin eluted at a concentration of ∼40% acetonitrile/water on a 0.5%/min gradient and was subsequently frozen at −80 °C followed by lyophilization. The resulting protein powder was determined in 0.01% (v/v) TFA. Concentrations of invaposin were determined by UV absorbance at 280 nm using the molar extinction coefficient of 14300 M^{-1} cm^{-1}. The molecular mass of invaposin was determined by mass spectrometry in linear mode using a 4700 Proteomic Analyzer MALDI-TOF/TOF mass spectrometer (Life Technologies, Darmstadt, Germany).

Assays for Membrane Permeabilizing Activity. Antimicrobial activity of invaposin was tested in two assays using *Bacillus megaterium* ATCC 14581 and *E. coli* ATCC 35218 as viable targets.[2] The minimal inhibitory concentration (MIC) against bacterial growth was determined by a microdilution susceptibility test with melittin as a positive control. Permeabilization of membranes of bacteria was assayed by monitoring the fluorescence of the DNA-binding dye SYTOX Green with cecropin P1 (100 nM) as a control peptide. Pore forming activity was followed by measuring fluorimetrically the dissipation of a valinomycin-induced membrane potential in liposomes prepared from crude soy bean phospholipids. The pore-forming peptide alamethicin (0.1 μM) was used as a positive control. The release of entrapped calcein from large unilamellar vesicles from 3:1 POPC/POPG (molar ratio), 3:1 POPC/POPA (molar ratio), 3:1 POPC/POPS (molar ratio), 3:1 POPC/CL (molar ratio), and 3:1 POPC/POPE (molar ratio) lipid mixtures, POPC, *E. coli* total, or polar lipid extract was assessed as described previously in detail.[2]

Liposome Preparation. The 3:1 POPC/POPG (molar ratio), 3:1 POPC/POPA (molar ratio), 3:1 POPC/POPS (molar ratio), 3:1 POPC/CL (molar ratio), or 3:1 POPC/POPE (molar ratio) lipid mixture, POPC, *E. coli* total, or polar lipid extract was dissolved in chloroform and subsequently evaporated under a stream of nitrogen to produce a thin lipid film. Residual solvent was removed by lyophilization, followed by rehydration for 2 h under continuous shaking in 20 mM sodium phosphate buffer (pH 6.0). The suspension was subjected to three freeze−thaw cycles using liquid nitrogen and a water bath at 37 °C. Finally, small unilamellar vesicles (SUVs) were produced by extrusion 21 times through 50 nm polycarbonate membranes (Avestin, Mannheim, Germany).

DOI: 10.1021/acs.biochem.5b00094
Biochemistry 2015, 54, 1778−1786

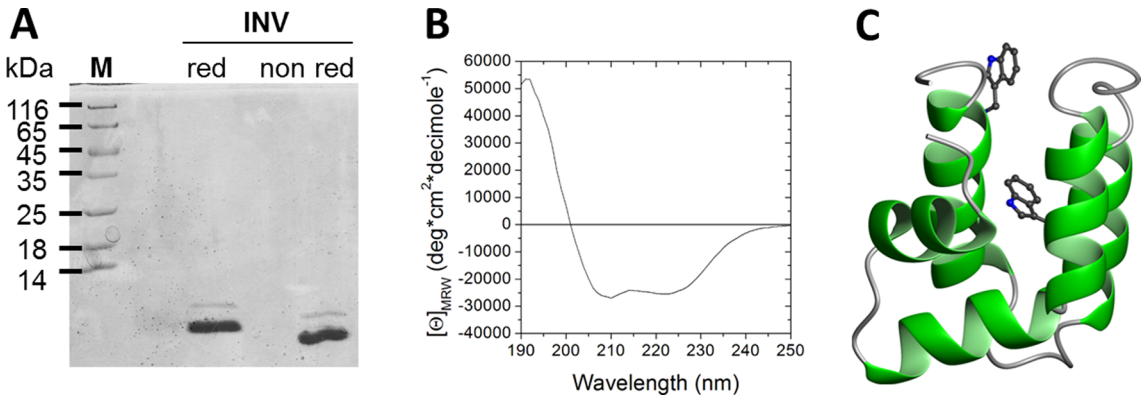

Figure 1. Purification and structural integrity of invaposin. (A) Sodium dodecyl sulfate−polyacrylamide gel electrophoresis analysis of purified invaposin (INV) under reducing (red) and nonreducing conditions (non red) showed bands at a position corresponding to the molecular mass of invaposin compared with the marker (M). (B) CD spectrum of invaposin in 0.01% TFA. (C) Model of invaposin depicted in ribbon representation with highlighted side chains of tryptophan residues. The picture was generated using MOLMOL.

Intrinsic Tryptophan Emission Fluorescence Spectroscopy. Tryptophan emission fluorescence measurements were performed on a Cary Eclipse fluorescence spectrometer (Varian) with an excitation wavelength of 290 nm at 20 °C. SUV lipid mixtures were added from 10 mg/mL stock solutions to a solution of invaposin (final concentration of 1 μM) in various buffers in quartz cuvettes with a path length of 1 cm (Hellma Analytics, Müllheim, Germany). After a short incubation, emission spectra were recorded from 300 to 450 nm, averaging three scans to create the final spectrum. Spectra were corrected for baseline and dilution after adding lipid vesicles for titration steps. Blue shifts were calculated from the emission maxima of protein and protein/lipid mixtures. The data of the tryptophan emission were fit sigmoidally using Origin 6.0.

The collisional quenching of tryptophan emission by water-soluble acrylamide was detected at an excitation wavelength of 290 nm in a similar setting as described before. From a 4.2 M acrylamide stock solution, aliquots were added in a stepwise manner (0 to 0.315 M) to a 1 μM protein solution in the absence and presence of 0.5 mM SUV lipid mixtures. Spectra were corrected for light scattering of the vesicles, dilution and baselines of the samples, containing no protein. The integrals of the emission spectra were analyzed using the Stern−Volmer equation:[27]

$$F_0/F = (1 + K_{sv}[Q])\exp(V[Q])$$

where F_0 and F are the fluorescence intensities in the absence and presence of quencher at concentration [Q], respectively, and V is a static quencher constant. The Stern−Volmer quenching constant K_{sv} facilitates the comparison of the quencher's accessibility to the tryptophan residues in aqueous solution or the membrane environment.

ANS Binding. The hydrophobic interaction of invaposin with the fluorescent dye 1-anilinonaphthalene-8-sulfonate (ANS) was analyzed on a Tecan Infinite Pro200 (Tecan, Crailsheim, Germany) fluorescence plate reader[28] for various pH and salt conditions. Protein or dye was loaded into a nonbinding 96-well plate (Greiner Bio One, Frickenhausen, Germany), pretreated with 0.1 mg/mL BSA at a concentration of 1 or 20 μM, respectively. ANS or invaposin was added in a stepwise manner, and the emission fluorescence intensity or maximum shift from 420 to 620 nm was measured after incubation in the dark for 30 min at room temperature with an excitation wavelength of 380 nm. The gain and z-parameter were kept constant for all experiments, and the fluorescence spectra were corrected for spectra of the respective buffers containing no protein. The integral of the curve was averaged from three measurements for each titration step and plotted against the concentrations of added molecules for the comparison of ANS−invaposin complexes.

Size-Exclusion Chromatography. Molecular size-exclusion chromatography was performed with 100 μg of invaposin at different pH values using a size-exclusion column (HiLoad Superdex 75 16/60 column, GE Healthcare) equilibrated with 20 mM sodium citrate buffer (pH 3.5), 20 mM sodium acetate buffer (pH 4.0, 4.25, 4.5, 5.0, and 5.5), or 20 mM Tris-HCl buffer (pH 7.5) at 4 °C. The column was calibrated by single runs of insulin (5700 Da), β-lactoglobulin (18300 Da), ovalbumin (41000 Da), and transferrin (81000 Da) (GE Healthcare) at a flow rate of 1 mL/min for each pH.

Circular Dichroism Spectroscopy. For the determination of secondary structural elements and changes upon lipid titration, circular dichroism spectroscopy (CD) was performed on a Jasco J-720 spectrometer (Jasco, Tokyo, Japan). Measurements of 5 μM invaposin in various buffers were conducted from 190 to 250 nm in a quarz cuvette with a path length of 1 mm at room temperature. The bandwidth was 2 nm, and four scans were averaged with a scanning speed of 20 nm/min. From each protein spectrum, the signal of the buffer was subtracted. For the addition of SUVs composed of different phospholipids, the spectra were corrected for further dilution. The secondary structure of invaposin was determined by using the spectral fitting method CONTIN/LL of the CDpro package.[29]

Dynamic Light Scattering. Dynamic light scattering (DLS) measurements were performed on a Laser-Spectroscatter 201 (RiNA, Berlin, Germany) at an angle of 90° and 22 °C. SUV suspensions (1 mM) were applied to 50 μM invaposin in 50 mM sodium actetate buffer (pH 4.0 and 5.0) and in 50 mM Tris-HCl buffer (pH 7.5), separately mixed carefully, and incubated for 5 min at room temperature. Subsequently, after centrifugation at 5000g and room temperature for 5 min, 10 μL was added to a quartz cuvette and the size distribution was monitored in 10 subsequent measurements. For data interpretation, particles with an occurrence of <0.1 were neglected.

DOI: 10.1021/acs.biochem.5b00094
Biochemistry 2015, 54, 1778−1786

Molecular Modeling. The molecular model of invaposin was generated by using the SWISS-Model server in fully automated mode.[30]

RESULTS

Recombinant Expression and Molecular Characterization of Invaposin. To analyze the lipid interactions of a defined single entity, we recombinantly expressed invaposin in *E. coli* and purified the protein to apparent homogeneity (Figure 1A). The molecular mass determined for the purified protein (m/z 8547.8) was in good agreement with the calculated mass (m/z 8547.6) provided that all six cysteine residues were involved in disulfide bonds.

To verify the structural integrity of the recombinant protein, we analyzed the overall secondary structure of recombinant invaposin by CD spectroscopy. The CD spectrum showed pronounced minima at 222 and 208 nm and a maximum at 192 nm characteristic of high α-helical content (Figure 1B). Despite rather low degrees of sequence similarity and clear differences in charge distribution when invaposin was compared to amoebapores, we still found the highest level of sequence identity among SAPLIPs in Blast searches with amoebapore A (28%) and used the tertiary structure of this protein as the template to model that of invaposin (Figure 1C). The helical content of 67% that we calculated from the model was very close to that of 60% estimated from CD measurements. In this model, the two tryptophan residues of invaposin were located either at the surface or in the center of the hydrophobic protein core.

Invaposin Does Not Permeabilize Membranes. Similar to the natural protein, recombinant invaposin (1 μM) did not display pore forming activity as judged by a liposome depolarization assay that measured whether a dissipation of a valinomycin-induced membrane potential in liposomes occurred, at two different pH values (5.2 and 7.4). Alamethicin was introduced in this assay as it represents the prototype of a pore-forming peptide. The release of calcein from lipid vesicles composed of a crude mixture of phospholipids was also not detectable. Moreover, we observed neither growth inhibiting activity up to 50 μM protein nor membrane permeabilizing activity toward viable bacteria using the more sensitive Sytox Green assay and 15 μM invaposin (data not shown).

Invaposin Binds to Lipid Membranes. As invaposin did not display antimicrobial activity, we analyzed by tryptophan emission fluorescence spectroscopy whether we can find evidence that invaposin interacts with lipid membranes at all. When purified invaposin encountered liposomes composed of various phospholipids, we observed fluorescence intensity increases and blue-shifted emission maxima (Figure 2A). At pH 3.5 and 4.0, remarkable shifts were measured for vesicles containing POPA and extracts of *E. coli* (11 and 12 nm, respectively). At the theoretically calculated pI of invaposin (pH 4.5) and above (pH 5.0–7.5), a lipid interaction was virtually not detectable. For zwitterionic POPC and POPC/POPE vesicles, no insertion of the tryptophan side chain could be observed, indicating a binding specificity of invaposin for anionic phospholipids under acidic pH conditions.

We also tested the lipid binding properties of invaposin toward SUVs in the presence of sodium chloride (150 mM) or bivalent cations such as calcium, magnesium, or zinc ions (10 mM). Under these conditions, the tryptophan emission fluorescence spectra did not change in the presence of lipids (not shown). Consequently, electrostatic interactions dominated the lipid binding properties of invaposin at acidic pH values.

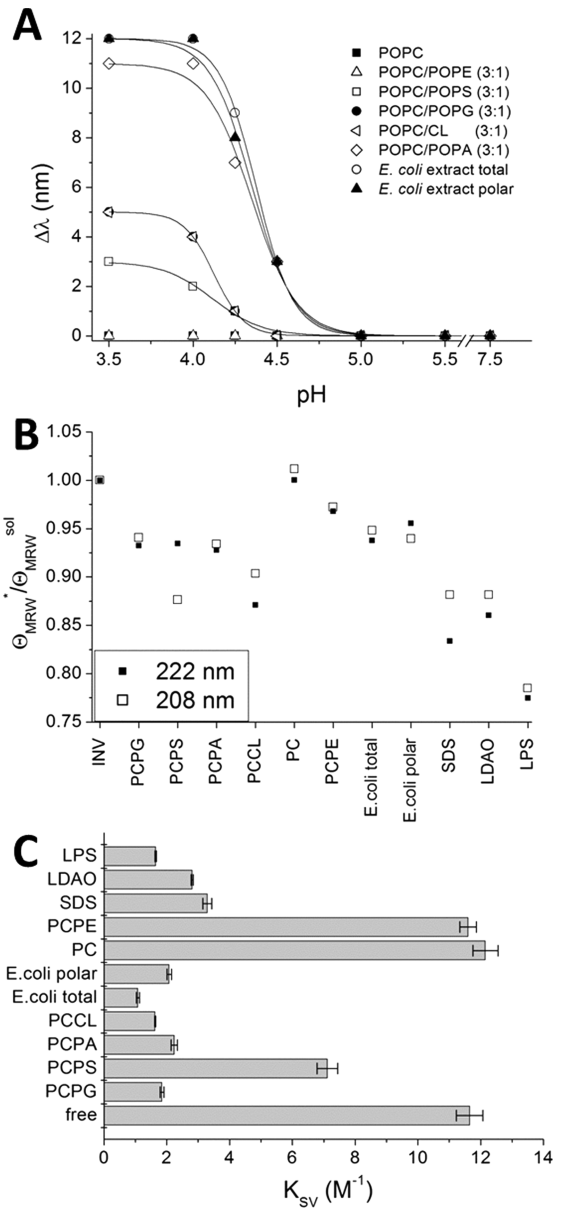

Figure 2. Lipid interactions of invaposin. (A) The shift of tryptophan emission fluorescence maxima was calculated for 1 μM invaposin in the presence of 0.5 mM phospholipid vesicles composed of various lipids at different pH values and referred to protein without lipids. (B) The ratio of ellipticities at 222 or 208 nm was calculated for 5 μM invaposin (INV) in the presence of various lipid vesicles at 250 μM (Θ_{MRW}*) composed of POPC and POPS (PCPS), POPC and POPA (PCPA), POPC and POPG (PCPG), POPC and cardiolipin (PCCL), POPC (PC), *E. coli* total (E. coli total), and polar (E. coli polar) lipid extract, or detergents (SDS, LDAO), and LPS compared to protein in solution (Θ_{MRW}^{sol}) by CD spectroscopy. (C) The Stern–Volmer quenching constants (K_{sv}) for 1 μM invaposin or in the presence of various lipid SUVs and micelle detergents were calculated by tryptophan emission fluorescence acrylamide quenching at pH 4.0. Error bars indicate deviations from curve fitting.

For the evaluation of overall secondary structural changes of invaposin upon lipid interaction, CD spectra were recorded at pH 4.0, where lipid interactions have been observed before (Figure 2B). The ratio of the characteristic α-helical signals at

DOI: 10.1021/acs.biochem.5b00094
Biochemistry 2015, 54, 1778–1786

222 and 208 nm in the presence of lipid vesicles or in solution was indicative of changes in the overall secondary structure of the protein upon lipid interaction. For all conditions tested, only minor effects on ellipticities could be observed (ratio of 0.8−1.0), suggesting minor secondary structural changes in association with lipid vesicles. In the presence of short acyl chain detergents such as SDS and LDAO, the ellipticities were in a range of experiments with POPC/POPS or POPC/CL vesicles. With LPS micelles, less pronounced ellipticities of the CD spectrum were observed, which represent the binding of invaposin to LPS accompanied by micellar conditions that were unlike those of detergent micelles or liposomes.

Next, we analyzed the localization of the tryptophan residues that participate in membrane binding by tryptophan emission fluorescence quenching in the presence of lipid vesicles composed of the same phospholipids or extracts analyzed in prior experiments (Figure 2C) at pH 4.0. The interaction of invaposin with SUVs containing anionic phospholipids (POPA, POPG, POPS, and cardiolipin) or *E. coli* lipid extracts was accompanied by small quenching constants indicating indole rings buried in the hydrophobic membrane. The direct correlation between protein−lipid interaction and tryptophan localization became apparent for invaposin in the presence of zwitterionic POPC or POPC/POPE vesicles where the quenching constants were in the range of the protein in solution, thereby indicating no lipid interaction.

Interaction of Invaposin with Short Chain Detergents. The interactions of SAP-C or SAP-A with SDS or LDAO have recently been shown to induce dramatic conformational changes and to lead to V-shaped open dimers of these proteins.[16,17] In this context, we analyzed the interaction of invaposin with LDAO (Figure 3A) and SDS (Figure 3B) in successive experiments. Even before the critical micelle concentration (cmc) of SDS (∼8 mM) or LDAO (∼1 mM), an insertion of the tryptophan residue was measured at pH 4.0 and 5.0 but not at pH 7.5. By the addition of sodium chloride, the cmc of SDS was reduced (∼1 mM)[31] and electrostatic interactions were disturbed. Here, an interaction of invaposin with detergents could still be observed.

Because NK-2, a peptide derivative from the SAPLIP NK-lysin, modulates the molecular assembly of lipopolysaccharide (LPS),[32,33] we tested whether we can find any evidence that invaposin also interacts with LPS under various pH conditions (Figure 3C). The tryptophan emission maxima showed a pronounced shift (11 nm) in the presence of LPS at pH 4.0, which resembles the pH optimum for the invaposin−lipid binding process. At pH 5.0 and 7.5, the binding of the protein to LPS was weaker as evidenced by smaller shifts of 7 and 4 nm, respectively. Here also, the addition of salts had no impact on the interaction of invaposin with LPS. These findings pointed again at a pH dependency of the lipid interaction of invaposin.

Invaposin Changes Its Conformation in a pH-Dependent Manner. To analyze whether pH-dependent changes in the overall secondary structure of invaposin already occur in the absence of lipids, we performed CD spectroscopic measurements of invaposin in solution at various pH values (Figure 4A). When we plotted the characteristic α-helical minima at 222 and 208 nm for each pH value (Figure 4B), we observed a decrease in ellipticity at pH 4.25 and 4.5, indicating an increase in α-helical content and thereby suggesting structural flexibility. At pH values below (pH 3.5−4.0) and above (pH 5.0−7.5) pH 4.5, the contents of α-helical elements were in similar ranges.

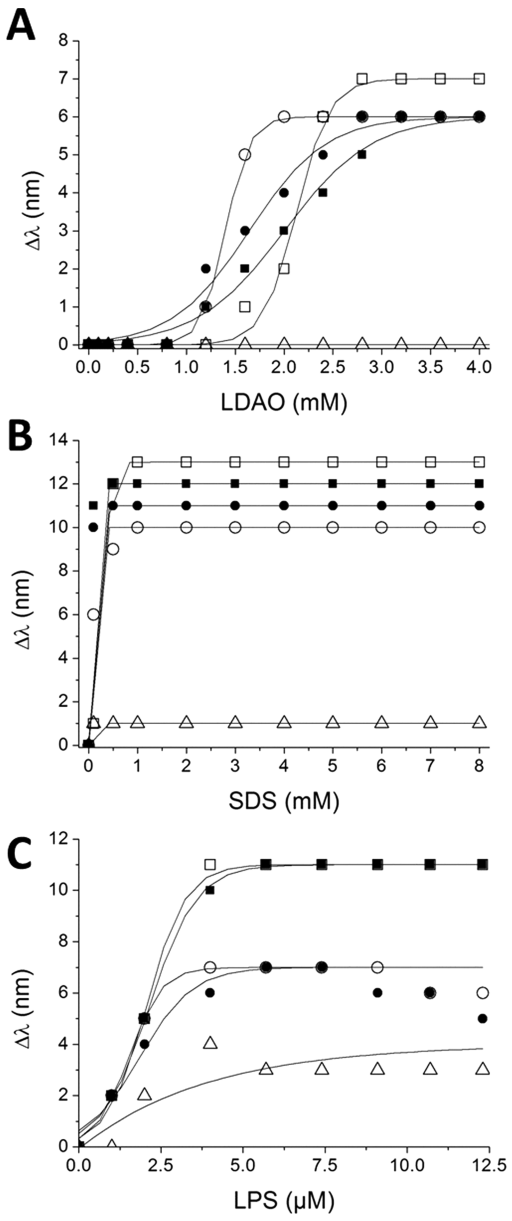

Figure 3. Interaction of invaposin with short chain detergents. The shifts of tryptophan emission fluorescence maxima were analyzed for 1 μM invaposin in the presence of increasing concentrations of (A) LDAO, (B) SDS, and (C) LPS at pH 4.0 (squares), 5.0 (circles), and 7.5 (triangles) in the absence (empty symbols) or presence of 150 mM NaCl (filled symbols).

In the model of invaposin, the tryptophan residues were presumably located either on the surface or in the core of the protein. Therefore, intrinsic tryptophan emission fluorescence quenching analysis was performed to determine the accessibility of the indole rings at different pH values by collisional acrylamide quenching (Figure 4C). The high Stern−Volmer quenching constants at pH 3.5 and 4.5 were attributed to the good accessibility of both tryptophans, indicating conformational changes at these two pH values. At other pH values, the lower quenching constants suggested that the core tryptophan residue was more buried.

To analyze whether a pH-dependent opening of the invaposin structure would allow an interaction with a hydrophobic molecule, the fluorescent probe ANS was

DOI: 10.1021/acs.biochem.5b00094
Biochemistry 2015, 54, 1778−1786

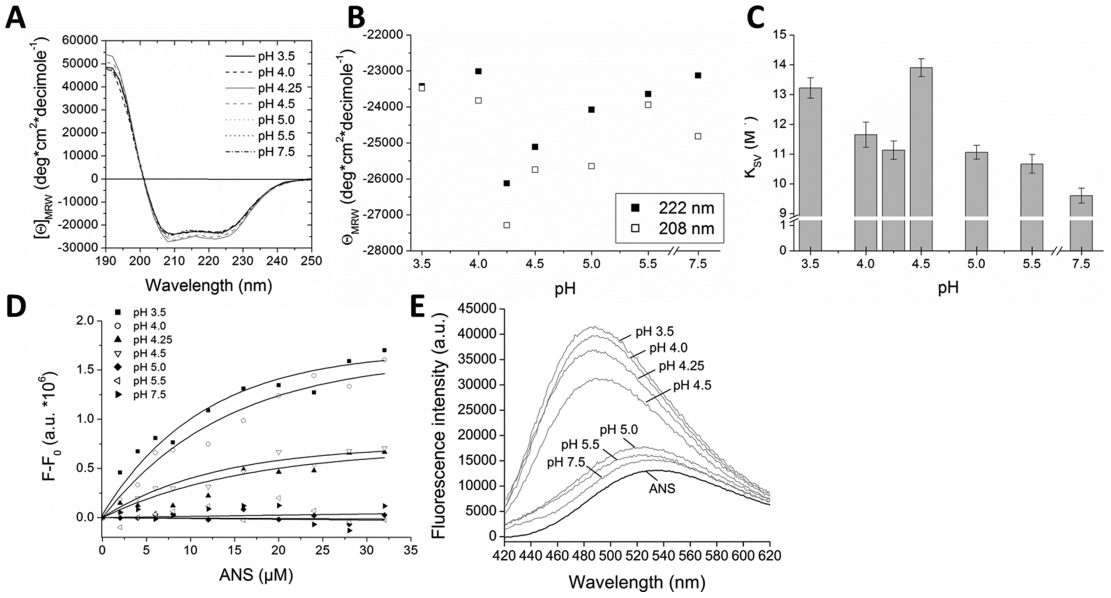

Figure 4. Structural changes and dimerization of invaposin upon acidification. (A) The CD spectra of invaposin in solution were recorded at various pH values. (B) The corresponding minima characteristic of α-helical contents (222 and 208 nm) were depicted for each pH value. (C) The Stern–Volmer quenching constants (K_{sv}) were calculated for 1 μM invaposin in the presence of increasing acrylamide concentrations at various pH. Error bars indicate deviations from curve fitting of experimental data. (D) The increase of fluorescence intensity (integral of the curve) was measured for the binding of increasing concentrations of ANS to 1 μM invaposin in solution at various pH values. Data were the mean of three experiments and fit with an exponential curve. (E) The maximal emission fluorescence shift of 20 μM ANS upon addition of 4.5 μM invaposin protein was depicted under all pH conditions tested. The fluorescence spectrum of the probe ANS was shown as the mean of all experiments.

incubated with invaposin at various pH values. In a first step, the successive binding of the probe to a constant concentration of protein (1 μM) was analyzed (Figure 4D). At pH 3.5–4.5, binding of ANS to invaposin was readily detectable as judged by an increase in fluorescence intensity. At pH 5.0–7.5, we did not observe an interaction. To test the inverse conditions, we added the protein to ANS (20 μM) and followed the emission fluorescence shift of the probe (Figure 4E). Here, the emission fluorescence shifts were maximal at pH 3.5, 4.0, and 4.25 (45 nm). At pH 4.5, the shift was less pronounced (41 nm) and weak association of the probe was observed at pH 5.0 (10 nm), 5.5 (8 nm), and 7.5 (5 nm), indicating a pH dependency of probe binding similar to that found before. As ANS is a sulfonic acid, we applied high concentrations of sodium chloride to disturb potential electrostatic interactions between the protein and ANS. The binding was comparable to that in the absence of salts (not shown). Therefore, we concluded that hydrophobic interactions were the predominant factor for protein–ANS binding and can be attributed to the accessibility of the core region of the protein at acidic pH.

Molecular Organization of Invaposin. We analyzed the molecular organization of invaposin by size-exclusion chromatography under identical conditions used before for CD spectroscopy (Figure 5). The retention of invaposin above pH 4.5 indicated monomers, whereas an assembly to dimers with various hydrodynamic volumes appeared to occur at more acidic pH values.

Vesicle Aggregation Induced by Invaposin. Fusogenic properties have been described for SAPLIPs such as SAP-C or the PSI.[34,35] Therefore, we analyzed the interaction of invaposin in the presence of SUVs composed of various phospholipids by DLS measurements at pH 4.0, 5.0, and 7.5 (Figure 6). Upon addition of invaposin at pH 4.0, vesicles with higher hydrodynamic radii were recorded for SUVs containing POPS, POPA, or POPG, which was in good agreement with

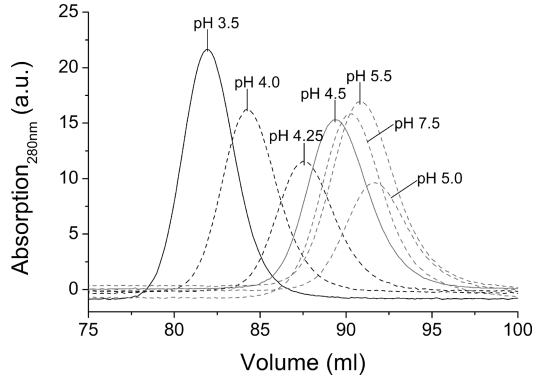

Figure 5. Molecular organization of invaposin. The elution profiles of invaposin were measured by size-exclusion chromatography at various pH.

the previous tryptophan emission fluorescence data. These aggregates were absent at pH 5.0 and 7.5, indicating again a pH-dependent lipid interaction of invaposin. Surprisingly, only minor effects were observed with vesicles containing cardiolipin or composed of *E. coli* total and polar lipid extracts, even at pH 4.0. These data point to various functions that were exerted by the protein upon membrane association. In the presence of zwitterionic lipids such as POPC, aggregation effects were not observed at any pH.

DISCUSSION

In this study, we analyzed the lipid interaction of a SAPLIP from the protozoon *E. invadens* for which virtually nothing was known about its activity and mode of action after it has been identified in amoebic extracts. The α-helical protein dimerizes under acidic pH conditions and becomes monomeric above pH 4.5 (pI of the protein). This monomer–dimer equilibrium is

DOI: 10.1021/acs.biochem.5b00094
Biochemistry 2015, 54, 1778–1786

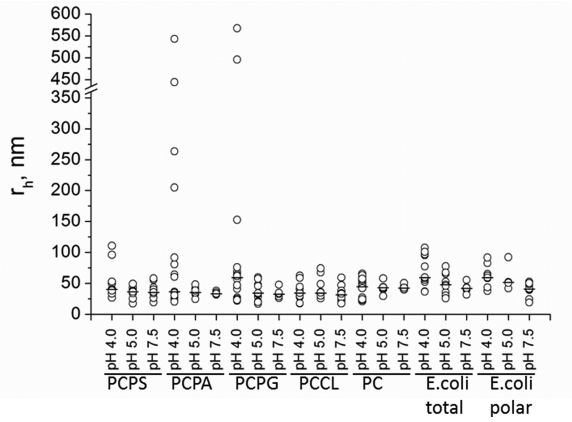

Figure 6. Lipid–vesicle aggregation induced by invaposin. DLS measurements were performed with 50 μM invaposin in the presence of 1 mM SUVs composed of POPC and POPS (PCPS), POPC and POPA (PCPA), POPC and POPG (PCPG), POPC and cardiolipin (PCCL), POPC (PC), *E. coli* total (E. coli total), and polar (E. coli polar) lipid extracts under various pH conditions. The hydrodynamic radii (r_h) of 10 measurements (○) and the corresponding median (black bars) are depicted.

similar to those of several anionic SAPLIP family members, e.g., human saposins A–D or the PSI from *Solanum tuberosum*.[14,17−19] According to the crystal structures of SAP-A–C and the PSI, the SAPLIP fold revealed an intrinsic conformational versatility induced by the presence of lipids, detergents, and acidic pH.[15−17,19] The latter conditions have been reported to be pivotal for the PSI to open its globular fold to a dimeric extended conformation as judged by in silico experiments.[36] Here, we performed fluorescence quenching and ANS binding experiments to demonstrate the accessibility of tryptophan residues and the arrangement of a hydrophobic pocket under acidic pH conditions, where invaposin appears as a dimer. The tryptophan residue in the core of invaposin is an adequate probe for the analysis of unfolding events from a globular to an extended tertiary structure. By using a combination of CD and tryptophan emission fluorescence spectroscopy, the accessibility of the indole ring due to minor changes of its secondary structural elements upon dimerization could be observed. A very similar result has been obtained by CD measurements of the PSI at pH 4.5 and 7.4.[18] Our results suggest that at low pH invaposin dimerizes and acquires an open conformation as known from human saposins.[15−17] Moreover, this extended dimeric conformation results in larger hydrodynamic volumes as evidenced by size-exclusion chromatography.

Under conditions at which it forms a dimer, invaposin exerts lipid binding preferences for anionic phospholipids (e.g., POPG, POPS, POPA, and cardiolipin) and *E. coli* extracts as determined by tryptophan emission fluorescence spectroscopy. This interaction is absent in the presence of NaCl, indicating electrostatic forces as the main driving force for invaposin–lipid binding. Additionally, the strong dependence of these lipid binding events on acidic pH suggests that the protein fulfills its function in an acidified compartment such as the lysosome and thereby resembles human saposins A–D.[1] The pH conditions that maximally support lipid interactions of SAP-B (pH 4.2),[26] SAP-C (pH 4.7),[34] or the PSI (pH 4.5)[18] are very close to that determined as the optimal pH value of invaposin (pH 4.0).

The interaction of invaposin with short acyl chain detergents such as negatively charged SDS or noncharged LDAO showed differences in the pH dependency and driving force as compared to the situation with phospholipids. Because at pH 5.0 an insertion of tryptophan side chains was still observable, the interaction appeared less restricted to low-pH conditions. Here, the addition of salts had no impact on the protein–detergent interaction, indicating that hydrophobic forces are essential for the interplay of protein and detergent. Comparable to the interaction of SAP-C with SDS micelles, the association of invaposin with the detergent was absent under basic pH conditions.[16] Therefore, a minimized protein–detergent model system can be used for further structural analysis.

As other SAPLIP members exert membrane permeabilization or leakage, we performed experiments with calcein-loaded vesicles and the SYTOX green assay toward bacteria such as *E. coli* and *B. megaterium*. Invaposin did not induce membrane permeabilization on model membranes or living bacteria. Additionally, invaposin exerted no antimicrobial activity even at high protein concentrations (50 μM), and the lowest pH possible in these experiments, i.e., pH 5.2. For some SAPLIP family members (Na-SLP-1, Ac-SLP-1, and Sap-B), it has been reported as well that no membrane perturbation was observed.[26,37] Together with the aggregating properties of invaposin, the data presented here point to a function comparable to that of SAP-B and SAP-C. The weak or reversible association of invaposin upon membrane interaction resembles mostly the mode of action of human SAP-B, known as a lipid solubilizer, which allows extraction of the phospholipid from whole membrane bilayers.[20] Conclusively, this work expands the known repertoire of SAPLIPs in amoeboid protozoans to include a protein that binds and extracts lipids from membranes without generating lytic pores. Presumably, invaposin allows solubilization of lipids from bacteria that have been engulfed by the amoeba. The strong interaction with LPS strengthens the notion that the protein acts upon acidification of the phagosome to dismantle the bacterial outer and cytoplasmic membranes and hence is relevant to the exploitation of microbes as a nutrient source.

AUTHOR INFORMATION

Corresponding Author

*Zoological Institute, Comparative Immunobiology, University of Kiel, Olshausenstrasse 40, 24098 Kiel, Germany. E-mail: mmichalek@zoologie.uni-kiel.de.

Author Contributions

M.M. and M.L. conceived the study, designed the experiments, and wrote the manuscript. M.M. performed experiments and analyzed the data.

Funding

This study was supported by the 'Cluster of Excellence Inflammation at Interfaces', Cluster laboratory X, of the German Research Foundation (DFG).

Notes

The authors declare no competing financial interest.

ACKNOWLEDGMENTS

We thank Heidrun Ließegang for technical assistance with the activity assays and Dr. Christoph Gelhaus for determining the molecular mass of the recombinant protein by matrix-assisted laser desorption ionization time-of-flight mass spectrometry measurements. We are grateful to Dr. Rosa Herbst and Veronika Haunerdinger for valuable contributions in the early phase of the project.

DOI: 10.1021/acs.biochem.5b00094
Biochemistry 2015, 54, 1778–1786

■ ABBREVIATIONS

SAPLIP, saposin-like protein; BSA, bovine serum albumin; CD, circular dichroism; ANS, 1-anilinonaphthalene-8-sulfonate; POPC, 1-palmitoyl-2-oleoyl-*sn*-glycero-3-phosphocholine; POPE, 1-palmitoyl-2-oleoyl-*sn*-glycero-3-phosphoethanolamine; POPG, 1-palmitoyl-2-oleoyl-*sn*-glycero-3-phospho(1′-*rac*-glycerol); POPS, 1-palmitoyl-2-oleoyl-*sn*-glycero-3-phospho-L-serine; POPA, 1-palmitoyl-2-oleoyl-*sn*-glycero-3-phosphate; CL, 1,1′,2,2′-tetraoleoyl cardiolipin; LPS, lipopolysaccharide; SUV, small unilamellar vesicle; LDAO, lauryldimethyl amine oxide; SDS, sodium dodecyl sulfate.

■ REFERENCES

(1) Kolter, T., Winau, F., Schaible, U. E., Leippe, M., and Sandhoff, K. (2005) Lipid-binding proteins in membrane digestion, antigen presentation, and antimicrobial defense. *J. Biol. Chem. 280*, 41125−41128.

(2) Bruhn, H., Riekens, B., Berninghausen, O., and Leippe, M. (2003) Amoebapores and NK-lysin, members of a class of structurally distinct antimicrobial and cytolytic peptides from protozoa and mammals: A comparative functional analysis. *Biochem. J. 375*, 737−744.

(3) Spiegel, R., Bach, G., Sury, V., Mengistu, G., Meidan, B., Shalev, S., Shneor, Y., Mandel, H., and Zeigler, M. (2005) A mutation in the saposin A coding region of the prosaposin gene in an infant presenting as Krabbe disease: First report of saposin A deficiency in humans. *Mol. Genet. Metab. 84*, 160−166.

(4) Kishimoto, Y., Hiraiwa, M., and O'Brien, J. S. (1992) Saposins: Structure, function, distribution, and molecular genetics. *J. Lipid Res. 33*, 1255−1267.

(5) Horowitz, M., and Zimran, A. (1994) Mutations causing Gaucher disease. *Hum. Mutat. 3*, 1−11.

(6) Nogee, L. M., Garnier, G., Dietz, H. C., Singer, L., Murphy, A. M., deMello, D. E., and Colten, H. R. (1994) A mutation in the surfactant protein B gene responsible for fatal neonatal respiratory disease in multiple kindreds. *J. Clin. Invest. 93*, 1860−1863.

(7) Leon, L., Tatituri, R. V., Grenha, R., Sun, Y., Barral, D. C., Minnaard, A. J., Bhowruth, V., Veerapen, N., Besra, G. S., Kasmar, A., Peng, W., Moody, D. B., Grabowski, G. A., and Brenner, M. B. (2012) Saposins utilize two strategies for lipid transfer and CD1 antigen presentation. *Proc. Natl. Acad. Sci. U.S.A. 109*, 4357−4364.

(8) Winau, F., Schwierzeck, V., Hurwitz, R., Remmel, N., Sieling, P. A., Modlin, R. L., Porcelli, S. A., Brinkmann, V., Sugita, M., Sandhoff, K., Kaufmann, S. H., and Schaible, U. E. (2004) Saposin C is required for lipid presentation by human CD1b. *Nat. Immunol. 5*, 169−174.

(9) Andersson, M., Gunne, H., Agerberth, B., Boman, A., Bergman, T., Sillard, R., Jornvall, H., Mutt, V., Olsson, B., Wigzell, H., et al. (1995) NK-lysin, a novel effector peptide of cytotoxic T and NK cells. Structure and cDNA cloning of the porcine form, induction by interleukin 2, antibacterial and antitumour activity. *EMBO J. 14*, 1615−1625.

(10) Pena, S. V., and Krensky, A. M. (1997) Granulysin, a new human cytolytic granule-associated protein with possible involvement in cell-mediated cytotoxicity. *Semin. Immunol. 9*, 117−125.

(11) Liepinsh, E., Andersson, M., Ruysschaert, J. M., and Otting, G. (1997) Saposin fold revealed by the NMR structure of NK-lysin. *Nat. Struct. Biol. 4*, 793−795.

(12) Anderson, D. H., Sawaya, M. R., Cascio, D., Ernst, W., Modlin, R., Krensky, A., and Eisenberg, D. (2003) Granulysin crystal structure and a structure-derived lytic mechanism. *J. Mol. Biol. 325*, 355−365.

(13) Hecht, O., Van Nuland, N. A., Schleinkofer, K., Dingley, A. J., Bruhn, H., Leippe, M., and Grötzinger, J. (2004) Solution structure of the pore-forming protein of *Entamoeba histolytica*. *J. Biol. Chem. 279*, 17834−17841.

(14) Rossmann, M., Schultz-Heienbrok, R., Behlke, J., Remmel, N., Alings, C., Sandhoff, K., Saenger, W., and Maier, T. (2008) Crystal structures of human saposins C and D: Implications for lipid recognition and membrane interactions. *Structure 16*, 809−817.

(15) Ahn, V. E., Faull, K. F., Whitelegge, J. P., Fluharty, A. L., and Prive, G. G. (2003) Crystal structure of saposin B reveals a dimeric shell for lipid binding. *Proc. Natl. Acad. Sci. U.S.A. 100*, 38−43.

(16) Hawkins, C. A., de Alba, E., and Tjandra, N. (2005) Solution structure of human saposin C in a detergent environment. *J. Mol. Biol. 346*, 1381−1392.

(17) Popovic, K., Holyoake, J., Pomes, R., and Prive, G. G. (2012) Structure of saposin A lipoprotein discs. *Proc. Natl. Acad. Sci. U.S.A. 109*, 2908−2912.

(18) Bryksa, B. C., Bhaumik, P., Magracheva, E., De Moura, D. C., Kurylowicz, M., Zdanov, A., Dutcher, J. R., Wlodawer, A., and Yada, R. Y. (2011) Structure and mechanism of the saposin-like domain of a plant aspartic protease. *J. Biol. Chem. 286*, 28265−28275.

(19) Ahn, V. E., Leyko, P., Alattia, J. R., Chen, L., and Prive, G. G. (2006) Crystal structures of saposins A and C. *Protein Sci. 15*, 1849−1857.

(20) Ciaffoni, F., Tatti, M., Boe, A., Salvioli, R., Fluharty, A., Sonnino, S., and Vaccaro, A. M. (2006) Saposin B binds and transfers phospholipids. *J. Lipid Res. 47*, 1045−1053.

(21) Andrä, J., Herbst, R., and Leippe, M. (2003) Amoebapores, archaic effector peptides of protozoan origin, are discharged into phagosomes and kill bacteria by permeabilizing their membranes. *Dev. Comp. Immunol. 27*, 291−304.

(22) Herbst, R., Ott, C., Jacobs, T., Marti, T., Marciano-Cabral, F., and Leippe, M. (2002) Pore-forming polypeptides of the pathogenic protozoon *Naegleria fowleri*. *J. Biol. Chem. 277*, 22353−22360.

(23) Eichinger, D. (1997) Encystation of *Entamoeba* parasites. *BioEssays 19*, 633−639.

(24) Herbst, R., Marciano-Cabral, F., and Leippe, M. (2004) Antimicrobial and pore-forming peptides of free-living and potentially highly pathogenic *Naegleria fowleri* are released from the same precursor molecule. *J. Biol. Chem. 279*, 25955−25958.

(25) Qi, X., and Grabowski, G. A. (2001) Differential membrane interactions of saposins A and C: Implications for the functional specificity. *J. Biol. Chem. 276*, 27010−27017.

(26) Remmel, N., Locatelli-Hoops, S., Breiden, B., Schwarzmann, G., and Sandhoff, K. (2007) Saposin B mobilizes lipids from cholesterol-poor and bis(monoacylglycero)phosphate-rich membranes at acidic pH. Unglycosylated patient variant saposin B lacks lipid-extraction capacity. *FEBS J. 274*, 3405−3420.

(27) Chang, Y. C., and Ludescher, R. D. (1994) Local conformation of rabbit skeletal myosin rod filaments probed by intrinsic tryptophan fluorescence. *Biochemistry 33*, 2313−2321.

(28) Penzer, G. R., Bennett, E. L., and Calvin, M. (1971) Isoleucyl-tRNA synthetase. A fluorescence study of the binding properties of the synthetase from *Escherichia coli*. *Eur. J. Biochem. 20*, 1−13.

(29) Sreerama, N., and Woody, R. W. (2000) Estimation of protein secondary structure from circular dichroism spectra: Comparison of CONTIN, SELCON, and CDSSTR methods with an expanded reference set. *Anal. Biochem. 287*, 252−260.

(30) Arnold, K., Bordoli, L., Kopp, J., and Schwede, T. (2006) The SWISS-MODEL workspace: A web-based environment for protein structure homology modelling. *Bioinformatics 22*, 195−201.

(31) Dutkiewicz, E., and Jakubowska, A. (2002) Effect of electrolytes on the physicochemical behaviour of sodium dodecyl sulphate micelles. *Colloid Polym. Sci. 280*, 1009−1014.

(32) Hammer, M. U., Brauser, A., Olak, C., Brezesinski, G., Goldmann, T., Gutsmann, T., and Andrä, J. (2010) Lipopolysaccharide interaction is decisive for the activity of the antimicrobial peptide NK-2 against *Escherichia coli* and *Proteus mirabilis*. *Biochem. J. 427*, 477−488.

(33) Brandenburg, K., Garidel, P., Fukuoka, S., Howe, J., Koch, M. H., Gutsmann, T., and Andrä, J. (2010) Molecular basis for endotoxin neutralization by amphipathic peptides derived from the α-helical cationic core-region of NK-lysin. *Biophys. Chem. 150*, 80−87.

(34) Qi, X., and Chu, Z. (2004) Fusogenic domain and lysines in saposin C. *Arch. Biochem. Biophys. 424*, 210−218.

DOI: 10.1021/acs.biochem.5b00094
Biochemistry 2015, 54, 1778−1786

(35) Egas, C., Lavoura, N., Resende, R., Brito, R. M., Pires, E., de Lima, M. C., and Faro, C. (2000) The saposin-like domain of the plant aspartic proteinase precursor is a potent inducer of vesicle leakage. *J. Biol. Chem. 275*, 38190−38196.
(36) De Moura, D. C., Bryksa, B. C., and Yada, R. Y. (2014) In silico insights into protein-protein interactions and folding dynamics of the saposin-like domain of *Solanum tuberosum* aspartic protease. *PLoS One 9*, e104315.
(37) Willis, C., Wang, C. K., Osman, A., Simon, A., Pickering, D., Mulvenna, J., Riboldi-Tunicliffe, A., Jones, M. K., Loukas, A., and Hofmann, A. (2011) Insights into the membrane interactions of the saposin-like proteins Na-SLP-1 and Ac-SLP-1 from human and dog hookworm. *PLoS One 6*, e25369.

DOI: 10.1021/acs.biochem.5b00094
Biochemistry 2015, 54, 1778−1786